Can volumetric ADC measurement help predict response to Y90 radioembolization in HCC?

Michael Vouche,[1] Riad Salem,[1,2,3] Robert J. Lewandowski,[1] Frank H. Miller[4]

[1]Section of Interventional Radiology and Division of Interventional Oncology, Department of Radiology, Robert H. Lurie Comprehensive Cancer Center, Northwestern University, Chicago, IL, USA

[2]Division of Hematology and Oncology, Department of Medicine, Robert H. Lurie Comprehensive Cancer Center, Northwestern University, Chicago, IL, USA

[3]Division of Transplantation, Department of Surgery, Comprehensive Transplant Center, Northwestern University, Chicago, IL, USA

[4]Department of Radiology, Feinberg School of Medicine, Northwestern Memorial Hospital, Northwestern University, 676 North Saint Clair Street Suite 800, Chicago, IL 60611, USA

Abstract

Aim: To compare changes in RECIST, anatomical volume, mRECIST, and volumetric diffusion-weighted Imaging parameters (3D apparent diffusion coefficient (ADC) measurements), with pathological analysis of hepatocellular carcinoma (HCC) treated by ^{90}Yttrium radioembolization (Y90). *Methods*: 21 patients were treated by Y90 as a sole treatment modality for solitary, >2 cm HCC that underwent liver transplantation. MRI at baseline, 1 and 3 months post-Y90, and tumor pathological findings on explants were reviewed in all patients. *Results*: Compared to baseline (RECIST/volume: 3.6 cm/17.7 cm^3), RECIST and volume were not modified after Y90 (1 month, $p = 0.28/0.09$ RECIST/tumor volume; 3 months, $p = 0.28/0.54$). In contrast, mRECIST (3.3–1.4 cm, $p < 0.001$), mean ADC (0.185–1.093 mm^2/s $\times 10^{-3}$, $p = 0.04$), and ADC standard deviation (STD) (0.041–0.201 mm^2/s $\times 10^{-3}$, $p = 0.0496$) changed as earlier as 1 month post-Y90. ADC STD % change was higher in ADC responding lesions than non-responding lesions at 1 month ($p = 0.002$) and 3 months ($p = 0.008$). All lesions exhibited necrosis on pathological analysis (11 partially viable, 10 complete pathological necrosis (CPN)) but no imaging criterion was able to predict CPN. mRECIST (±ADC) at 1 ($\kappa \pm$ ADC = 0.08/0.06) or 3 months ($\kappa = -0.06/-0.06$) were poor predictors of pathological response. *Conclusion*: As soon as 1 month post-treatment, mRECIST and volumetric ADC performed better than traditional size RECIST or volumetric parameters in detecting imaging response to Y90; however, CPN cannot be predicted by any criteria. Improvements in methodologies to assess response and identification of better surrogates are awaited.

Key words: Hepatocellular carcinoma—Radioembolization—Yttrium-90—Response assessment—ADC

ADC	Apparent diffusion coefficient
cTACE	Conventional transarterial chemoembolization
CPN	Complete pathological necrosis
DWI	Diffusion-weighted imaging
GRE (m)	Gradient echo
RECIST	(Modified) response criteria in solid tumors
MRI	Magnetic resonance imaging
IQR	Interquartile range
^{99}Tc-MAA	^{99}Technetium-macroaggregated albumin
STD	Standard deviation
Y90	^{90}Yttrium radioembolization

Despite continuous breakthroughs in technical and clinical knowledge on liver-directed therapies, response assessment still needs improvement. Initially, tumor response of solid tumors by cross-sectional imaging to

Correspondence to: Frank H. Miller; *email:* fmiller@northwestern.edu

antitumoral therapies was assessed by size criteria: bi-(World Health Organization criteria) then unidimensional (Response Criteria in Solid Tumors criteria (RECIST)) measurements of the entire tumor [1]. Modified Response Criteria in Solid Tumors (mRECIST), looking at changes in tumor enhancement and necrosis by unidimensional measurement, have more recently been considered for response assessment of HCC after liver-directed therapies [2]. However, despite simple methodology and consistency, mRECIST face limitations as those criteria do not take into consideration physiologic patterns of response and are supported by a limited number of studies with pathological assessment [3–5]. Moving forward in the era of functional imaging, new response criteria have to incorporate microscopic changes affecting both tumor and surrounding parenchyma, and need to take into consideration the tumor type and treatment modalities. As a consequence, simple anatomical criteria such as RECIST or mRECIST, based on size or enhancement, do not always reflect true tumoricidal effect of these therapies. Diffusion-weighted imaging (DWI), providing information on cell membrane integrity and cellular density, has been hypothesized to improve and predict response assessment [6, 7]. In addition, volumetric delineation may replace uni/bidimensional measurements as imaging software and spatial resolution of imaging modalities evolve [2, 8, 9]. Beyond conventional mean apparent diffusion coefficient (ADC), volumetric ADC measurement provides more realistic tumor delineation compared to uni- or bi-dimensional approaches, and permits analyzing tumor response heterogeneity by generating histograms from voxel-by-voxel ADC values calculation [10–12]. The aim of the present study was to correlate changes in different anatomical (RECIST, anatomical volume), enhancement (mRECIST), and DWI parameters with post-transplant pathological analysis, and to discuss the added value of mRECIST and volumetric DWI combination for the response assessment of HCC after [90]Yttrium radioembolization (Y90).

Materials and methods

Patient sample

This retrospective radiological-pathological study was in compliance with the Health Insurance Portability and Accountability Act. Institution Review Board approval was obtained. No financial support was obtained for this study. Imaging and pathological results of all patients treated by Y90 and transplanted between September 2004 and April 2013 at our institution were reviewed. The post-Y90 imaging follow-up policy at our institution includes an abdominal MRI scan at 1 and 3 months post-treatment. Inclusion criteria limited the study to patients (1) with solitary HCC > 2 cm and proven by biopsy or imaging (AASLD guidelines) [13], (2) treated by selective

or lobar Y90 only, (3) not previously treated by any liver-directed therapies (4) who ultimately underwent orthotopic liver transplantation. Out of 57 patients who fulfilled those criteria, 36 were excluded from the final analysis because (1) transplantation occurred before the 3 month scan (11 patients excluded), (2) transplantation occurred before the 1 month scan (2 excluded), (3) the 3 month scan had not been performed (2 excluded), (4) the baseline scan was a CT scan (6 excluded), (5) no DWI sequences or ADC map had been performed at baseline or at follow-up (6 excluded), (6) magnetic resonance imaging (MRI) sequences could not be analyzed on the dedicated software because of compatibility issues (3 excluded), (7) unacceptable imaging artifacts rendered measurement inaccurate (6 excluded). In summary, 21 patients were available for complete analysis, who were scanned between December 2005 and August 2012.

Y90 radioembolization and dosimetry

Patients were treated on an outpatient basis using a selective segmental or lobar treatment with glass microspheres loaded with [90]Yttrium (TheraSphere, Nordion, Ottawa, Canada) by experienced interventional radiologists (second and third authors, >15 years as Interventional Radiologists, >10 years of experience in Y90 radioembolization), according to previously published recommendations and guidelines [14, 15]. Treatments were preceded by a planning angiogram during which parasitizing arteries were embolized, catheter tip positioning was optimized, and [99]Technetium-macroaggregated albumin (^{99}Tc-MAA) was infused in order to estimate pulmonary and gastro-intestinal shunting.

MRI acquisition

All studied patients had undergone abdominal MRI scans prior to Y90 (baseline scan), and then at 1 and 3 months post-treatment (follow-up scans). Scans were performed on 1.5-T MRI units (Magnetom Avanto or Espree; Siemens AG, Munich, Germany) using a liver protocol comprising transverse and coronal single-shot turbo spin echo T2-weighted half Fourier acquisitions (HASTE), multiple dynamic three-dimensional gradient echo (GRE) T1-weighted sequences (VIBE) with spectral fat suppression performed before and after intravenous administration by a power injector (Spectris; Medrad Warrendale, PA) of 0.1 mmol/kg Gadopentate dimeglumine and Gadobutrol (Magnevist and Gadovist; Bayer HealthCare Pharmaceuticals, Berlin, Germany) followed by 20 mL saline flush (2 mL/s). Post-contrast acquisitions were obtained at arterial (based on fluoro-preparation sequence), portal venous (70 s) and multiple delayed phases (2–10 min). Diffusion-weighted sequences were also performed, using breath-hold multishot fast spin echo echo-planar technique, with 6-mm slice thickness, 90° flip

Table 1. Differences in diffusion scan parameters according to year

	2005–2006	2007	2008–2010	2011–2012
b value	0, 500	50, 500	50, 500, 1000	50, 500, 800
Number of averages	2			4

angle, TR/TE of approximately 5000/80, bandwidth of 1446 Hz/Px, and parallel imaging factor of 2. The chosen *b* values and other parameters were gradually changed during the 6 years included in the study (Table 1).

Post-processing and imaging parameters

ADC values per voxel were generated using the multiple *b* values and presented on an ADC map. All series of each baseline and follow-up MRI scans were transferred in Digital Imaging and Communications in Medicine (DICOM) format to a PACS workstation (Centricity PACS; General Electric, Milwaukee, WI) and to a dedicated software (Versavue; iCAD, Nashua, NH) permitting volumetric tumor delineation and data analysis. Longest tumor diameter in the transverse plane (cm), maximal diameter of tumor enhancing portions in the transverse plane (cm), and tumor volume (cm^3) were acquired by manual delineation on the T1-weighted post-contrast at the arterial phase (considering non-enhancing tissue on arterial phase as non-tumoral tissue). For the measurement of enhancing tumor portions, a thin and continuous peripheral rim of enhancement was not considered to be of tumoral nature as this observation is typically a post-Y90 observance. A three-dimensional manual delineation of tumor margins (based on diffusion restriction) was performed on the ADC map in order to generate volumetric voxelwise ADC measurements. As spatial resolution of ADC maps is inferior to other acquired sequences, the decision was made to guide the volumetric tumor delineation by co-registering other series (T1 pre-/post-contrast, DWI low/high *b* value images) and delineating areas suspicious of tumor (arterial enhancement, diffusion restriction). The tumor volume on ADC maps, as well as the mean and standard deviation (STD) of ADC values measured in this volume, were reported.

Imaging and pathological response assessment

By imaging, partial response to therapy was defined from baseline as a ≥30% reduction for the maximal diameter in the transverse plane according to the RECIST criteria; as a ≥30% reduction for the maximal diameter of tumor enhancing portions in the transverse plane according to mRECIST criteria and as a reduction ≥65% of the tumor volume (volumetric transformation of RECIST criteria) [1, 2, 16]. Complete response was defined as the absence of visible tumor (for RECIST and Volume criteria) or the absence of enhancing tumor portions (for mRECIST). A ≥15% increase in mean ADC value was considered as cut-off to assess response using ADC [10, 17]. Pathological analysis of explants consisted in a gross examination, followed by a thin slicing (0.5–1.0 cm) of representative samples and hematoxylin and eosin staining. The presence of necrosis and of viable tissue inside the tumor was systematically reported by experienced pathologists. Reports of pathological analyses of explants were carefully reviewed by the primary author and tumors were classified as completely necrotic (complete pathological necrosis (CPN)), partially viable (incomplete necrosis with persistence of tumor tissue) or completely viable (persistence of tumor tissue without necrosis).

Statistics

Patients' and lesions' characteristics were presented using descriptive statistics (mean ± SD) for normal distribution, median, and range for non-normal distribution. The Wilcoxon test was used to compare values of imaging parameters pre- and post-treatment. Tumors were classified as responder (complete or partial response) or non-responder by ADC or pathological criteria as previously specified. Imaging parameters (% change between responding and non-responding lesions) were compared at 1 and 3 months using the Mann–Whitney test. Radiological classification was compared between CPN and non-CPN lesions using the Fisher's exact test for categorical variable. Weighted kappa agreement coefficient was also calculated between imaging response at 1 month, 3 months, and pathological classification. All statistics were conducted on MedCalc (Mariakerke, Belgium). A *p* value was considered significant if <0.05 and as a trend if ≥0.05 but <0.10.

Results

Patients and lesions characteristics

Selected patients included 14 males and 7 females. Their median (IQR) age was 58.5 years old (57.5–63.0). The diagnosis of HCC was confirmed by imaging for 14 patients and by biopsy for 7 patients. Y90 glass microspheres were infused in a segmental artery for 14 patients and in a lobar artery for 7 patients. None of the patients had been previously treated by systemic or liver-directed therapy. No other type of therapy was administered before liver transplantation. Median (IQR) cumulative doses administered at the treatment site were 111.55 Gy (80.97–146.62). Delays (IQR) were 27.0 days (12.0–41.0) between baseline scan and treatment date, 32.0 days (28.8–35.0) between treatment date and 1 month scan, 94.0 days (86.8–116.5) between treatment date and 3 months scan and 177.0 days (51.5–218.3) between 3 months scan and transplant date.

Table 2. Imaging measurements at baseline, 1 month and 3 months post-Y90

	Baseline	1 Month	3 Months	p value (Wilcoxon test)		
				Baseline to 1 month	Baseline to 3 months	1–3 months
RECIST (cm)	3.6 (2.7–4.6)	3.7 (2.8–5.4)	3.5 (2.1–4.9)	0.28	0.28	0.05
mRECIST (cm)	3.3 (2.9–5.1)	1.4 (0.8–3.2)	1.2 (0.5–2.2)	<0.001	<0.001	0.10
Anatomical Volume (cm^3)	17.7 (8.4–40.6)	24.3 (6.5–60.4)	16.1 (4.0–59.4)	0.09	0.54	0.11
ADC Volume (cm^3)	18.0 (8.2–47.6)	22.6 (10.0–63.4)	18.3 (3.8–43.2)	0.20	0.20	0.03
Mean ADC (mm^2/s $\times$ 10^{-3})	0.185 (0.118–1.092)	1.93 (0.159–1.316)	0.926 (0.157–1.309)	0.04	0.03	0.69
STD ADC (mm^2/s $\times$ 10^{-3})	0.041 (0.023–0.220)	0.201 (0.039–0.272)	0.164 (0.034–0.280)	0.0496	0.09	0.85

$N = 21$
Values presented as median and interquartile range (IQR)
ADC, Apparent diffusion coefficient; STD, standard deviation

Table 3. ADC STD % change in ADC R/NR

	ADC R ($n = 13$)	ADC NR ($n = 8$)	Total	p value
ADC STD % change				
1 Month	660.6 (44.6–896.8)	−9.0 (−88.8–12.5)	51.3 (0.6–756.2)	0.002
3 Months	83.3 (24.8–1018.2)	−9.1 (−55.4–6.8)	30.5 (−8.5–705.05)	0.008

ADC, Apparent diffusion coefficient; R, responder; NR, non-responder; STD, standard deviation

Imaging changes (Tables 2 and 3)

Baseline scans and follow-up scans at 1 and 3 months were available and were reviewed for all patients included in the study ($N = 21$). Appropriate measurements were properly obtained for every studied imaging parameter. Compared to baseline (median RECIST = 3.6 cm; tumor volume = 17.7 cm^3), median RECIST and tumor volume measurements did not change significantly after 1 month (3.7 cm, $p = 0.28$; 24.3 cm^3, $p = 0.09$) or 3 months (3.5 cm, $p = 0.28$; 16.1 cm^3, $p = 0.54$) despite a trend of reduction using RECIST criteria from the 1 to 3 months follow-up ($p = 0.05$). mRECIST reduced from baseline (3.3–1.4 cm, $p < 0.001$) while mean ADC increased significantly at 1 month (0.185–1.093 mm^2/s $\times$ 10^{-3}, p = 0.04), those changes being maintained at 3 months (1.2 cm, $p < 0.001$ and 0.926 mm^2/s $\times$ 10^{-3}, $p = 0.03$). STD (standard deviation) of ADC increased significantly at 1 month (0.041–0.201 mm^2/s $\times$ 10^{-3}, $p = 0.0496$), suggesting an increased dispersion of voxelwise ADC values. ADC STD % change was higher in responding lesions by ADC than non-responding lesions at 1 month (660.6% vs. −9.0%, $p = 0.002$) and 3 months (83.3 vs. −9.1, $p = 0.008$) post-treatment. However, this observation was not related to a difference in ADC responding versus non-responding lesions (median [IQR]: 112.8 [77.8–117.4] vs. 109.1 Gy [89.1–191.0], $p = 0.5$).

Prediction of pathological response by imaging parameters (Table 4)

All lesions exhibited necrosis on pathological analysis and were classified as partially viable ($n = 11$) or CPN ($n = 10$). No difference in imaging parameters at baseline or in their percentage change at 1 or 3 months was observed between CPN and partially viable tumors. For a baseline ADC mean cut-off of 0.2 mm^2/s $\times$ 10^{-3}, there was no difference in CPN rate in lower ADC mean (5/13) compared to higher ADC mean (5/8) (bilateral Chi-Square test, $p = 0.1827$).

Radiological-pathological classification (Table 5) and agreement between imaging response at 1 month, 3 months, and pathological response (Table 6)

No criterion was able to detect complete pathological necrosis (CPN). mRECIST and ADC were the imaging parameters classifying the most lesions as responding at 1 and 3 months. Despite slight improvement of agreement between 1 and 3 months imaging assessment by adding 3D ADC analysis to mRECIST non-responders ($\kappa = 0.38$–0.49), mRECIST ($\pm$ADC) at 1 ($\kappa \pm$ ADC = 0.08/0.06) or 3 months ($\kappa = -0.06/-0.06$) were poor predictors of pathological response.

Discussion

The aims of the study were to evaluate the usefulness and to discuss advantages and limitations of 3D ADC parameters (mean and STD) in comparison (RECIST/anatomical volume/mRECIST) or combination (mRECIST) to conventional radiological response criteria in predicting pathological response of solitary HCC after Y90.

Size and enhancement criteria

In the present study, size criteria (RECIST and anatomical volume) showed clear limitations in detecting early (1 month) response, some of them being inherent

Table 4. % Change of imaging measurements in CPN and partially viable tumor based on pathology

	CPN ($N = 10$)	Partially viable ($N = 11$)	p value
RECIST			
Baseline (cm)	3.3 (2.5 to 4.4)	4.0 (3.0 to 5.1)	0.28
% change 1 month	6.9 (0.0 to 10.9)	0.0 (−13.8 to 14.2)	0.50
% change 3 months	−15.9 (−35.0 to 30.8)	−12.5 (−31.5 to −4.6)	0.72
mRECIST			
Baseline (cm)	3.2 (2.5 to 4.2)	3.7 (3.2 to 7.4)	0.16
% change 1 month	−28.6 (−76.7 to 3.0)	−67.6 (−86.5 to −11.8)	0.44
% change 3 months	−63.9 (−80.8 to −52.0)	−61.3 (−95.9 to −40.1)	0.62
Anatomical volume			
Baseline (cm^3)	12.3 (6.7 to 38.8)	20.3 (11.0 to 54.4)	0.23
% change 1 month	20.4 (−34.3 to 54.5)	0.0 (−21.7 to 18.9)	0.53
% change 3 months	−20.5 (−69.3 to 98.6)	−38.3 (−58.8 to −8.8)	0.62
Mean ADC			
Baseline ($mm^2/s \times 10^{-3}$)	0.553 (0.121 to 1.091)	0.178 (0.118 to 0.948)	0.94
% change 1 month	38.2 (9.1 to 633.6)	18.2 (−15.0 to 840.8)	0.94
% change 3 months	30.1 (−11.6 to 93.3)	22.8 (−1.5 to 771.8)	0.94
ADC STD (in mean ADC R/NR)			
Baseline ($mm^2/s \times 10^{-3}$)	0.097 (0.037 to 0.216)	0.027 (0.016 to 0.189)	0.16
% change 1 month	13.7 (0.7 to 534.6)	63.8 (−9.5 to 788.8)	0.67
% change 3 months	19.0 (−21.7 to 67.3)	83.3 (−4.8 to 916.8)	0.44

ADC, Apparent diffusion coefficient; CPN, complete pathological necrosis; R, responder; NR, non-responder

to the treatment's nature. Ablative techniques such as radiofrequency ablation immediately destroy tissues, leaving in place a coagulated cavity larger than the baseline tumor while a major component of conventional transarterial chemoembolization (cTACE) mechanism is the brutal hypoxia caused by the entrapment of embolic particles in the arterial feeding vessels [18, 19]. One of the earliest imaging surrogates of this mechanism is a precocious and persistent decrease in enhancement within minutes after treatment, followed by necrosis and delayed decrease in size [20]. The size of Y90 microspheres is smaller than embolic agents used in bland embolization or cTACE (up to 20–30 μm in diameter for glass microspheres), with the microsphere being trapped in the arteriolar capillaries and causing less hypoxia in targeted tissues [18]. The main effect of Y90 is now known to be the selective exposure of the tumor and the surrounding parenchyma to very high-dose radiation therapy. As a consequence, while it also causes necrosis and size changes, these macroscopic features may be delayed compared to bland embolization or cTACE despite effective therapy. [21–24] Unlike other transarterial therapies, a radiation-induced inflammatory response is generally observed in the treated area, leading to difficulties to distinguish residual or recurrent tumor from inflammation in cases of persistent enhancement [3, 24]. Intratumoral septa can also show patterns of enhancement after treatment and may contribute to a delay in imaging manifestations of response [21]. Hence, despite a clear response according to mRECIST observed as early as 1 month post-Y90, we recognize that mRECIST, postulating that all enhancing tissue in treated tumors corresponds to viable tumoral tissue, is still suboptimal [2].

3D ADC

Kamel et al. published extensively on methodological refinement and potential applications of ADC in hepatic tumors treated by locoregional therapies and were the first to develop the use of 3D ADC in this setting [6, 10–12, 16, 17, 25]. Results from their studies suggest that ADC is an earlier surrogate of response compared to size criteria [6]. A survival benefit was demonstrated in cholangiocarcinoma treated by TACE and in neuroendocrine liver metastases treated by intraarterial therapy exhibiting response by ADC [10, 11]. One of their study focused on the identification of volumetric functional response criteria of unresectable HCC treated by intraarterial therapy and confirmed that 3D ADC parameters permit to stratify survival [16]. However, to our knowledge, no study explored the use of 3D ADC on a pure population of HCC treated by Y90 only.

In the present study, volumetric ADC (cell density/membrane permeability) was also found to be dramatically modified early after Y90 at 1 and 3 months, suggesting a potential to detect tumor response earlier than RECIST criteria and anatomical volume measurements (Table 2) [26]. However, on the contrary to results obtained by Manelli et al. in a population of HCC treated by chemoembolization suggesting that baseline ADC is a prognostic factor of pathological outcome, our study failed to demonstrate the utility of baseline ADC mean as a predictor of CPN [27]. There remain methodological issues to address concerning the use of 3D ADC. For instance, would a manual or an automated segmentation tool be more adapted? A better inter-observer agreement was recently observed using semi-automated volumetric ADC measurements compared with the manual drawing of volumes of

Table 5. Radiological–pathological classification

	1 Month				3 Months			
	CR	PR	NR	*p* value	CR	PR	NR	*p* value
RECIST								
CPN	0	0	10	1.0	0	2	8	1.0
Partially viable	0	0	11		0	2	9	
mRECIST								
CPN	2	3	4	0.8	2	6	2	1.0
Partially viable	1	6	5		3	7	1	
Anatomical volume								
CPN	0	1	9	1.0	0	3	7	0.6
Partially viable	0	1	10		0	2	9	

	1 Month			3 Months		
	R	NR	*p* value	*R*	NR	*p* value
ADC						
CPN	7	3	0.7	7	3	0.7
Partially viable	6	5		6	5	

ADC, Apparent diffusion coefficient; CPN, complete pathological necrosis; CR, complete response (by imaging); NR, non-responder (by imaging); PR, partial response (by imaging)

Table 6. One to three months radiological and radiological-pathological agreements

	CPN Pathology	Partially viable	No necrosis	κ (strength)	CR	PR	NR	κ (strength)
1 Month mRECIST					3 months mRECIST			
CR (*n* = 3)	2	1	0	0.06 (poor)	2	1	0	0.38 (fair)
PR (*n* = 9)	3	6	0		3	6	0	
NR (*n* = 9)	5	4	0		0	6	3	
Total (*n* = 21)	10	11	0		5	13	3	
1 Month mRECIST + ADC					3 months mRECIST + ADC			
CR (*n* = 3)	2	1	0	0.08 (poor)	2	1	0	0.49 (moderate)
PR (*n* = 14)	6	8	0		3	11	0	
NR (*n* = 4)	2	2	0		0	2	2	
Total (*n* = 21)	10	11	0		5	14	2	
3 Months mRECIST								
CR (*n* = 5)	2	3	0	−0.06 (poor)				
PR (*n* = 13)	6	7	0					
NR (*n* = 3)	2	1	0					
Total (*n* = 21)	10	11	0					
3 Months mRECIST + ADC								
CR (*n* = 5)	2	3	0	−0.06 (poor)				
PR (*n* = 13)	7	7	0					
NR (*n* = 3)	1	1	0					
Total (*n* = 21)	10	11	0					

ADC, Apparent diffusion coefficient; CPN, complete pathological necrosis, CR, complete response (by imaging); NR, non-responder (by imaging); PR, partial response (by imaging)

interest for the treatment response of HCC after cTACE and drug-eluting beads TACE [25]. However, the use of (semi-)automated software might be less adapted to Y90. Indeed, as already mentioned, tumor margins are often poorly demarcated after Y90, as surrounding parenchyma is also exposed to radiation-induced alterations, limiting automated segmentation performances. As demonstrated by Mannelli et al. and Kim et al. in HCC treated by cTACE, contrast-enhanced MRI with subtraction technique, particularly the arterial phase, is valuable for estimating intratumoral necrosis and considered to be more consistent than ADC for the detection of pathological necrosis [28, 29]. However, this is dependent on lack of respiratory misregistration, which can be difficult in such a patient population. Continuous improvement in dedicated software will increase volumetric delineation accuracy. Refinements in automated segmentation, motion correction, deformable coregistration, and subtraction reconstruction (for instance, subtraction between arterial and pre-contrast sequences) would be particularly beneficial [30]. Improvements in spatial resolution of DWI sequences could allow isovoxel ADC maps that would improve ADC measurements.
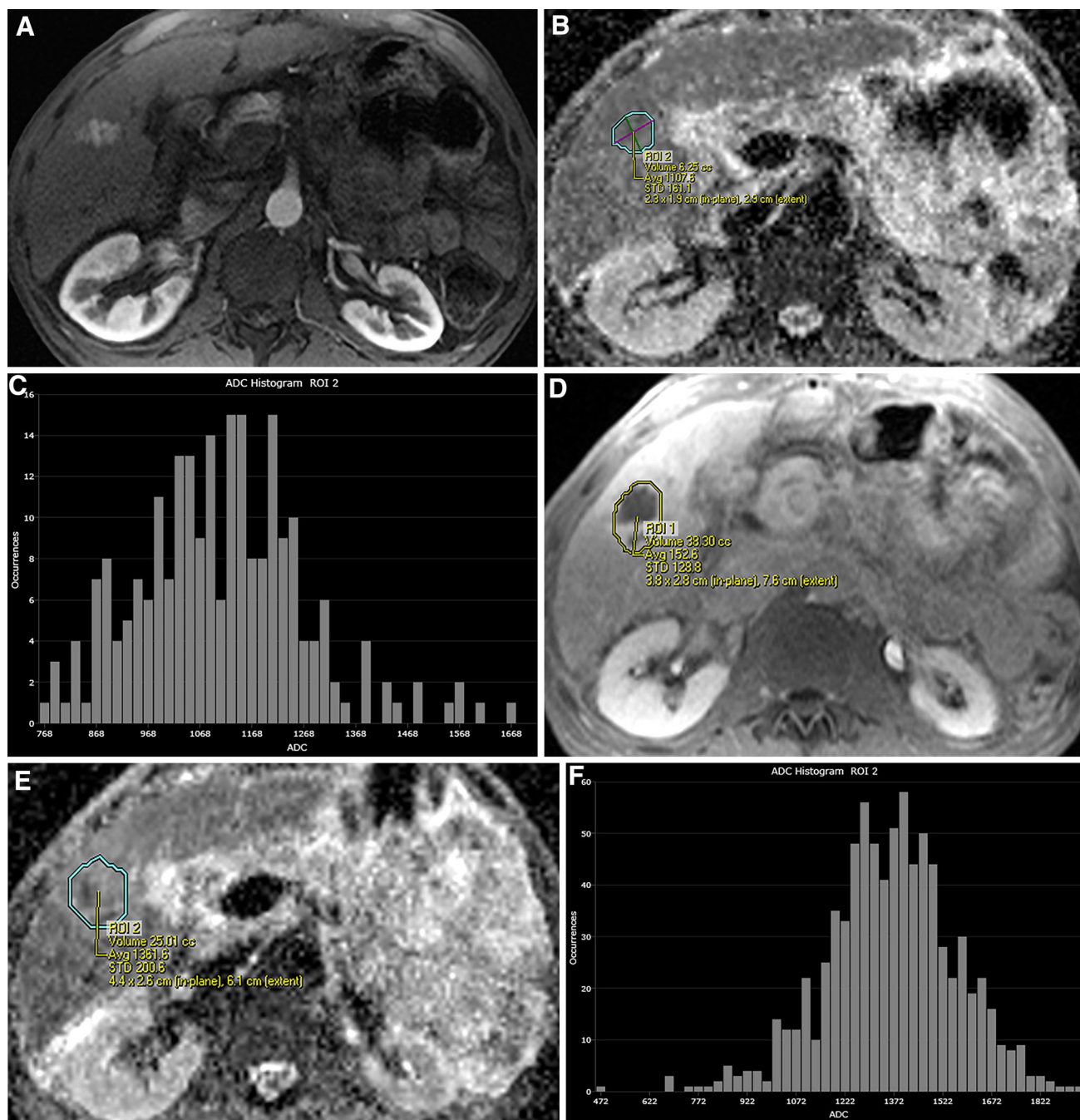
Fig. 1. A small hepatocellular carcinoma showing typical patterns of arterial enhancement on axial T1 fat suppressed contrast-enhanced image (**A**) and restricted diffusion on ADC map (**B**) with histogram presentation (**C**) was treated by Y90. Post-treatment MRI scans shows liver heterogeneity with increased size, enhancing borders, and necrosis, decrease in enhancing tumor burden, and increased mean and STD of ADC values at 1 month (**D**, **E**, and **F**) (1.362 and 0.201 mm^2/s $\times$ 10^{-3}) and 3 months (**G**, **H**, and **I**) (*bottom row*, 1.417 and 0.270 mm^2/s $\times$ 10^{-3}) compared to baseline (1.108 and 0.161 mm^2/s $\times$ 10^{-3}). On pathological examination, this lesion was found to be completely necrotic without persistent neoplasm.

Intratumoral ADC heterogeneity

Another approach to detect post-treatment imaging changes is to focus on post-Y90 intratumoral heterogeneity. A potential cause of this phenomenon is a non-uniform distribution of radioactive microspheres [31].

Response heterogeneity is still poorly understood but may play an important role in treatment success estimation. In order to improve the radiological response assessment by ADC, the use of volumetric delineation tools appears particularly adapted after transarterial therapies. In the
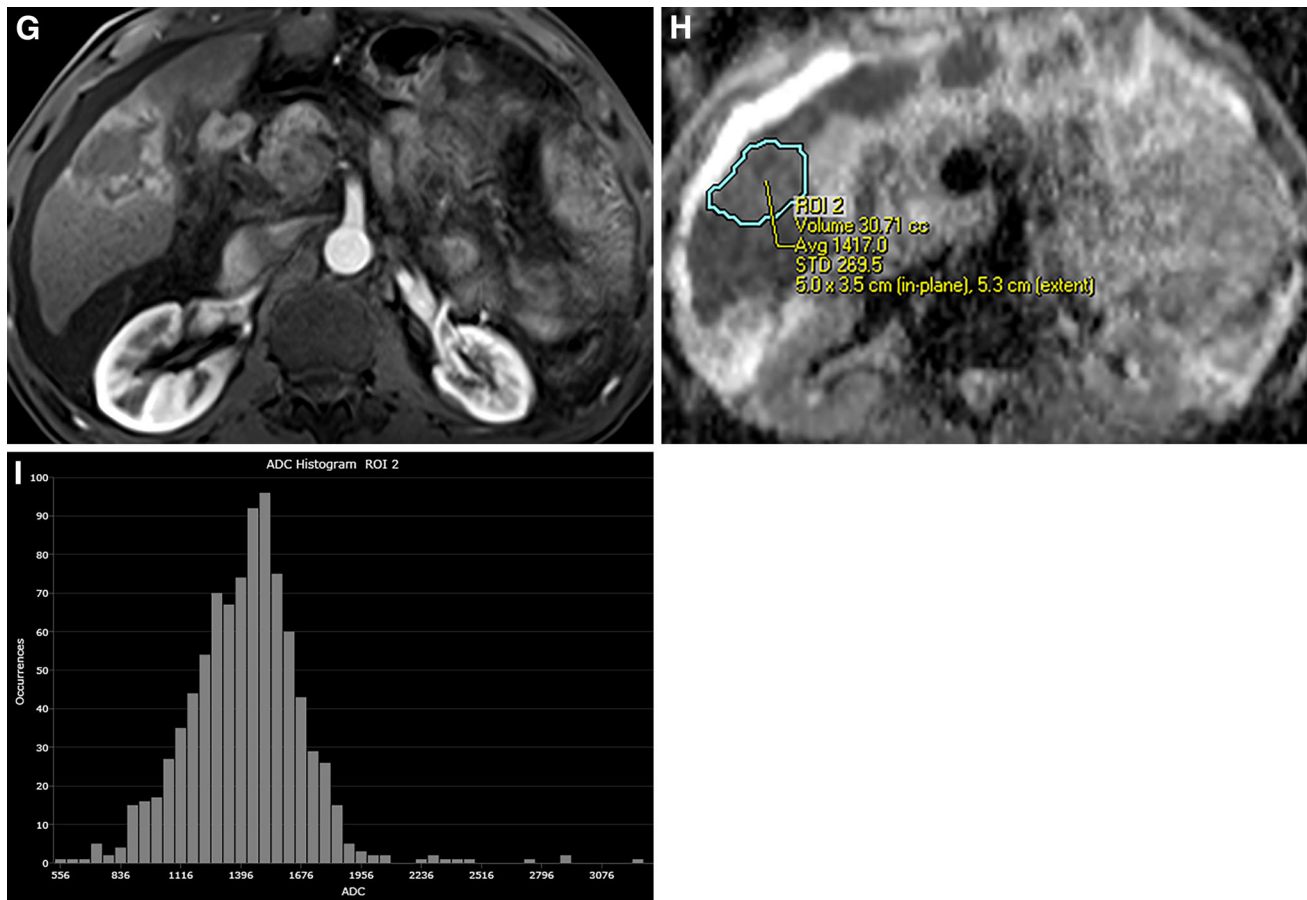
Fig. 1. continued

present study, histogram presentation of data permitted to analyze the heterogeneity inside volumes of interest, and a clear increase of ADC STD was observed after Y90, particularly when mean ADC was increased (Table 3). This suggests greater heterogeneity of water diffusion restriction after treatment, possibly mixed patterns of necrosis, membrane disruption, and reduction of cellularity (facilitated water molecules diffusion), contrasting with areas of persistent tumor and inflammation (restricted diffusion) (Fig. 1).

mRECIST and ADC combination

Combining mRECIST and ADC improved concordance between 1 and 3 months imaging follow-up from "fair" ($\kappa = 0.38$) to "average" ($\kappa = 0.49$) but did not correspond to more accurate interpretation of pathological results (Table 6). This is in accordance with Bonekamp et al. who demonstrated survival benefit if combining volumetric enhancement and ADC criteria after conventional and drug-eluting-beads TACE for unresectable HCC [16]. However, we limited our analysis to pathological correlation and not survival benefits as our patients had transplants.

Limitations of pathological analysis

A reduction of the tumor burden was confirmed by pathological analysis: all lesions ($n = 21$) exhibited various degrees of necrosis, 10/21 being completely necrotic. The presence of necrosis can be confidently attributed to therapy, spontaneous necrosis of HCC only being reported in case reports describing large and rapidly growing HCC or in association with arterial feeder thrombosis [32, 33]. As a consequence, mRECIST and mean ADC are suspected to be earlier markers of pathological response. However, despite being considered a gold standard in tumor response assessment, pathological analysis has its own limitations. For instance, the detection of the complete absence of viable tumoral tissue (CPN) was recently found to be unpredictable by imaging at 1 or 3 months following Y90 [4]. Concordantly, despite equivalent baseline characteristics, no difference in imaging parameters or their percentage change could be observed between CPN and partially viable tumors in the present study (Table 4). This issue has recently been considered in a consensus panel on transcatheter therapies for hepatic malignancies [34]. Radiation cellular damage is a heterogeneous and dynamic process inducing early (necrosis) or

delayed (apoptosis) death, impaired cell metabolism without death (sideration) or blocked cell replication. Hence, cytological examination on the explant itself is probably not entirely representative of the total treatment effect. Comparable radiological–pathological discrepancies leading to treatment effect underestimation have been described after radiofrequency ablation for HCC [35]. Consequently, the best approach for radiological–pathological interpretation would imply acquiring a complementary scan on the date of transplant but this is generally not feasible.

Limitations and strengths

As objective limitations of this study, we recognize the retrospective design of the study, the small patient sample, variable b values for DWI, and the lack of standardized methodology for obtaining 3D ADC measurement. The present study is however one of the few radiological–pathological studies considering a pure population of HCC treated by Y90 with explants and the first to apply volumetric ADC measurements in such a population. This is of particular interest as ADC interpretation remains limited and lacks validation endpoints, particularly related to post-Y90 therapy. In our study, we selected HCC lesions that were single, small and easily delineated before treatment, providing an interesting model for a response assessment study.

Conclusion

mRECIST and volumetric ADC were more effective than traditional size criteria (RECIST) or volumetric size in detecting an imaging response to Y90 and deserve consideration. mRECIST and ADC changes occurred as soon as 1 month post-Y90 when no response was seen with size criteria even at the 3 month scans. However, both mRECIST and volumetric ADC face severe methodological limitations in the response assessment of HCC treated by Y90. Improvements in methodologies and identification of better surrogates are still awaited.

References

1. Eisenhauer EA, Therasse P, Bogaerts J, et al. (2009) New response evaluation criteria in solid tumours: revised RECIST guideline (version 1.1). Eur J Cancer 45(2):228–247. doi:10.1016/j.ejca.2008.10.026
2. Lencioni R, Llovet JM (2010) Modified RECIST (mRECIST) assessment for hepatocellular carcinoma. Seminars Liver Dis 30(1):52–60. doi:10.1055/s-0030-1247132
3. Riaz A, Kulik L, Lewandowski RJ, et al. (2009) Radiologic-pathologic correlation of hepatocellular carcinoma treated with internal radiation using yttrium-90 microspheres. Hepatology 49(4):1185–1193. doi:10.1002/hep.22747
4. Vouche M, Kulik L, Atassi R, et al. (2013) Radiological-pathological analysis of WHO, RECIST, EASL, mRECISTand DWI: imaging analysis from a prospective randomized trial of Y90±sorafenib. Hepatology 22(10):26487
5. El-Gazzaz G, Sourianarayanane A, Menon KV, et al. (2013) Radiologic-histological correlation of hepatocellular carcinoma treated via pre-liver transplant locoregional therapies. Hepatobiliary Pancreat Dis Int 12(1):34–41
6. Kamel IR, Reyes DK, Liapi E, Bluemke DA, Geschwind JF (2007) Functional MR imaging assessment of tumor response after 90Y microsphere treatment in patients with unresectable hepatocellular carcinoma. J Vasc Interv Radiol 18(1 Pt 1):49–56. doi:10.1016/j.jvir.2006.10.005
7. Rhee TK, Naik NK, Deng J, et al. (2008) Tumor response after yttrium-90 radioembolization for hepatocellular carcinoma: comparison of diffusion-weighted functional MR imaging with anatomic MR imaging. J Vasc Interv Radiol 19(8):1180–1186. doi:10.1016/j.jvir.2008.05.002
8. Lin M, Pellerin O, Bhagat N, et al. (2012) Quantitative and volumetric European Association for the Study of the Liver and Response Evaluation Criteria in Solid Tumors measurements: feasibility of a semiautomated software method to assess tumor response after transcatheter arterial chemoembolization. J Vasc Interv Radiol 23(12):1629–1637. doi:10.1016/j.jvir.2012.08.028
9. Yaghmai V, Miller FH, Rezai P, Benson AB 3rd, Salem R (2011) Response to treatment series: part 2, tumor response assessment–using new and conventional criteria. AJR Am J Roentgenol 197(1):18–27. doi:10.2214/ajr.11.6581
10. Halappa VG, Bonekamp S, Corona-Villalobos CP, et al. (2012) Intrahepatic cholangiocarcinoma treated with local-regional therapy: quantitative volumetric apparent diffusion coefficient maps for assessment of tumor response. Radiology 264(1):285–294. doi:10.1148/radiol.12112142
11. Gowdra Halappa V, Corona-Villalobos CP, Bonekamp S, et al. (2013) Neuroendocrine liver metastasis treated by using intraarterial therapy: volumetric functional imaging biomarkers of early tumor response and survival. Radiology 266(2):502–513. doi:10.1148/radiol.12120495
12. Li Z, Bonekamp S, Halappa VG, et al. (2012) Islet cell liver metastases: assessment of volumetric early response with functional MR imaging after transarterial chemoembolization. Radiology 264(1):97–109. doi:10.1148/radiol.12112161
13. Sherman M, Bruix J, Porayko M, Tran T (2012) Screening for hepatocellular carcinoma: the rationale for the American Association for the Study of Liver Diseases recommendations. Hepatology 56(3):793–796. doi:10.1002/hep.25869
14. Salem R, Thurston KG (2006) Radioembolization with 90Yttrium microspheres: a state-of-the-art brachytherapy treatment for primary and secondary liver malignancies: part 1: technical and methodological considerations. J Vasc Interv Radiol 17(8):1251–1278
15. Kennedy A, Nag S, Salem R, et al. (2007) Recommendations for radioembolization of hepatic malignancies using yttrium-90 microsphere brachytherapy: a consensus panel report from the radioembolization brachytherapy oncology consortium. Int J Radiat Oncol Biol Phys 68(1):13–23. doi:10.1016/j.ijrobp.2006.11.060
16. Bonekamp S, Li Z, Geschwind JF, et al. (2013) Unresectable hepatocellular carcinoma: MR imaging after intraarterial therapy. Part I. Identification and validation of volumetric functional response criteria. Radiology 268(2):420–430. doi:10.1148/radiol.13122307
17. Corona-Villalobos CP, Pan L, Halappa VG, et al. (2013) Agreement and reproducibility of apparent diffusion coefficient measurements of dual-b-value and multi-b-value diffusion-weighted magnetic resonance imaging at 1.5 Tesla in phantom and in soft tissues of the abdomen. J Comput Assist Tomogr 37(1):46–51. doi:10.1097/RCT.0b013e3182720e07
18. Kritzinger J, Klass D, Ho S, et al. (2013) Hepatic embolotherapy in interventional oncology: technology, techniques, and applications. Clin Radiol 68(1):1–15. doi:10.1016/j.crad.2012.06.112
19. Kim YS, Lee WJ, Rhim H, et al. (2010) The minimal ablative margin of radiofrequency ablation of hepatocellular carcinoma (>2 and <5 cm) needed to prevent local tumor progression: 3D quantitative assessment using CT image fusion. AJR Am J Roentgenol 195(3):758–765. doi:10.2214/ajr.09.2954

20. Wang D, Gaba RC, Jin B, et al. (2011) Intraprocedural transcatheter intra-arterial perfusion MRI as a predictor of tumor response to chemoembolization for hepatocellular carcinoma. Acad Radiol 18(7):828–836. doi:10.1016/j.acra.2011.02.016

21. Atassi B, Bangash AK, Bahrani A, et al. (2008) Multimodality imaging following 90Y radioembolization: a comprehensive review and pictorial essay. Radiographics 28(1):81–99. doi:10.1148/rg.28 1065721

22. Miller FH, Keppke AL, Reddy D, et al. (2007) Response of liver metastases after treatment with yttrium-90 microspheres: role of size, necrosis, and PET. AJR Am J Roentgenol 188(3):776–783. doi:10.2214/ajr.06.0707

23. Guo Y, Yaghmai V, Salem R, et al. (2013) Imaging tumor response following liver-directed intra-arterial therapy. Abdom Imaging 38(6):1286–1299. doi:10.1007/s00261-013-0017-5

24. Ibrahim SM, Nikolaidis P, Miller FH, et al. (2009) Radiologic findings following Y90 radioembolization for primary liver malignancies. Abdom Imaging 34(5):566–581. doi:10.1007/s00261-008-9454-y

25. Bonekamp D, Bonekamp S, Halappa VG, et al. (2014) Interobserver agreement of semi-automated and manual measurements of functional MRI metrics of treatment response in hepatocellular carcinoma. Eur J Radiol 83(3):487–496. doi:10.1016/j.ejrad.2013.11.016

26. Riaz A, Miller FH, Kulik LM, et al. (2010) Imaging response in the primary index lesion and clinical outcomes following transarterial locoregional therapy for hepatocellular carcinoma. JAMA 303(11):1062–1069. doi:10.1001/jama.2010.262

27. Mannelli L, Kim S, Hajdu CH, Babb JS, Taouli B (2013) Serial diffusion-weighted MRI in patients with hepatocellular carcinoma: prediction and assessment of response to transarterial chemoembolization. Preliminary experience. Eur J Radiol 82(4):577–582. doi:10.1016/j.ejrad.2012.11.026

28. Mannelli L, Kim S, Hajdu CH, et al. (2009) Assessment of tumor necrosis of hepatocellular carcinoma after chemoembolization: diffusion-weighted and contrast-enhanced MRI with histopathologic correlation of the explanted liver. AJR Am J Roentgenol 193(4):1044–1052. doi:10.2214/ajr.08.1461

29. Kim S, Mannelli L, Hajdu CH, et al. (2010) Hepatocellular carcinoma: assessment of response to transarterial chemoembolization with image subtraction. J Magn Reson Imaging 31(2):348–355. doi:10.1002/jmri.22038

30. Duke E, Deng J, Ibrahim SM, et al. (2010) Agreement between competing imaging measures of response of hepatocellular carcinoma to yttrium-90 radioembolization. J Vasc Interv Radiol 21(4):515–521. doi:10.1016/j.jvir.2009.11.020

31. Walrand S, Hesse M, Chiesa C, Lhommel R, Jamar F (2014) The low hepatic toxicity per Gray of 90Y glass microspheres is linked to their transport in the arterial tree favoring a nonuniform trapping as observed in posttherapy PET imaging. J Nucl Med 55(1):135–140. doi:10.2967/jnumed.113.126839

32. Yokoyama T, Yoshida H, Hirakata A, et al. (2012) Spontaneous complete necrosis of advanced hepatocellular carcinoma. J Nippon Med Sch 79(3):213–217

33. Sasaki T, Fukumori D, Yamamoto K, et al. (2013) Management considerations for purported spontaneous regression of hepatocellular carcinoma: a case report. Case Reports Gastroenterol 7(1):147–152. doi:10.1159/000350501

34. Brown DB, Gould JE, Gervais DA, et al. (2009) Transcatheter therapy for hepatic malignancy: standardization of terminology and reporting criteria. J Vasc Interv Radiol 20(7 Suppl):S425–S434. doi:10.1016/j.jvir.2009.04.021

35. Cho YK, Kim Y, Rhim H (2009) Pitfalls in the radiological and pathological correlation of tumour response rates of hepatocellular carcinoma following radiofrequency ablation. J Clin Pathol 62(12):1071–1073. doi:10.1136/jcp.2009.069716